Biochemistry

 Volume 38, Number 33 August 17, 1999

Articles

Thermal Sensitivity of the Red Absorption Tail of the Photosystem II Reaction Center Complex†

Laura Finzi, Giuseppe Zucchelli, Flavio Massimo Garlaschi, and Robert Charles Jennings*

Dipartimento di Biologia, Universita' degli Studi di Milano and Centro CNR Biologia Cellulare e Molecolare delle Piante, Via Celoria 26, 20133 Milano, Italy

Received March 11, 1999; Revised Manuscript Received June 2, 1999

ABSTRACT: The red tail of the absorption spectrum of the D1−D2−cyt*b*559 complex, defined as the absorption signal not described by the two Gaussian sub-bands associated with the intense electronic transitions at 680 and 683 nm, exhibits anomalous temperature behavior. This tail was analyzed in the temperature interval between 80 and 300 K in terms of the mean square deviation (σ^2) of the total Q_y absorption band and by Gaussian sub-band decomposition. The value of the average optical reorganization energy ($S\nu_m$) obtained from the temperature dependence of σ^2 for the whole absorption band was 32 cm^{-1}, and changed to 16−20 cm^{-1} after subtraction of the sub-bands describing the red tail. This latter value is in agreement with the hole burning literature data for chlorophyll bound to proteins, and indicates that the rather high value for the apparent optical reorganization energy obtained by analysis of the total Q_y band of the D1−D2−cyt*b*559 complex is determined by the temperature sensitivity of the red tail. This suggests that the long wavelength absorption tail might be due to vibrational transitions associated with vibrational modes in the range of 80−150 cm^{-1} which are thermally accessible and give rise to an absorption signal on the low-energy side of the (0,0) transition. On the basis of this assumption, the electron−phonon coupling strength (*S*) for these modes is estimated to be in the range 0.028−0.18. This interpretation furthermore supports the idea that the electronic transition near 683 nm is that of a monomer chlorophyll.

In photosystem II of higher plants, photochemistry occurs at the reaction center where the primary donor (P680) reduces the primary acceptor (pheophytin) with a time constant which is thought to be between 2 and 3 ps (*1*, *2*). A relatively stable chlorophyll (chl)−protein complex which binds both the primary donor and acceptor in a functionally active state was isolated by Chapman (*3*). This complex, known as D1−D2−cyt*b*559, binds six chlorophyll *a* and two pheophytin molecules (for a review, see refs *4* and *5*). These pigments bind to nonequivalent protein sites and give rise to considerable spectral congestion in the wavelength interval between 660 and 684 nm, thus complicating interpretation of the D1−D2−cyt*b*559 absorption spectrum. Nonetheless, several individual transitions have been tentatively identified. The two pheophytins may absorb near 670 (*6*) and 680 nm (*7*−*9*), respectively, and it is generally accepted that the primary donor also absorbs near 680 nm (*7*−*10*). Absorption difference spectroscopy in selectively photobleached complexes, hole burning, and CD spectroscopy indicate the presence of a transition near 674 nm (*5*, *9*, *11*, *12*), while a comparative analysis of the five and six chlorophyll binding preparations

† This work was in part financed by the MURST grant with project code 9705150034_004 and title "Fotoinibizione: meccanismi molecolari e meccanismi di protezione".

10.1021/bi990568o CCC: $18.00
Published on Web 07/29/1999

suggests that there is another chl absorption near 670 nm (*5*).

Finally, Kwa et al. (*13*) and Chang et al. (*5*) with absorption and triplet-minus-singlet studies at liquid helium temperature showed the presence of a low-energy transition in the D1−D2−cyt*b*559 complex near 683−684 nm. Konermann et al. (*14*), using site selection vibrational fluorescence spectroscopy, demonstrated that this transition is associated with a chlorophyll rather than a pheophytin molecule, and its inhomogeneously broadened band was recently analyzed at 80 K by Finzi et al. (*11*).

There is some discussion in the literature concerning the electron−phonon coupling properties of the long wavelength absorbing pigments in the D1−D2−cyt*b*559 complex which is relevant to the question of whether these pigments are to be considered as part of a primary donor multimer (*15*, *16*). Extensive hole burning studies by Small and co-workers (*17*) have shown that the electron−phonon coupling to low-frequency phonon modes ($\nu_m = 20-30$ cm^{-1}) is strong (S, coupling strength, ≥ 2) for the primary donors of both bacterial and plant photosystems, while that of monomeric, antenna-like chlorophylls is rather weak ($S \leq 1$). For the transition around 683 nm, both hole burning (*18*) and selective photobleaching (*11*) studies suggest values for S in the range of 0.7−0.9. On the other hand, site-selected fluorescence studies of the red tail of this complex have been interpreted in terms of a quite strong "average" electron−phonon coupling strength ($S \cong 1.6$) of the red-most electronic transition to a number of Franck−Condon active phonon modes in the frequency range from 20 to 500 cm^{-1}, implying that the 683 nm transition may in fact form part of a primary donor chlorophyll multimer (*19*). In addition, we have previously noted, using the absorption band thermal broadening approach to analyze electron−phonon coupling (*20*), that the red absorption tail of the D1−D2−cyt*b*559 complex can be described by a broad Gaussian sub-band, near 680 nm, though this requires that it be assigned with unreasonably high electron−phonon coupling values. Even though this broad band is not considered to have any precise physical meaning, this observation is interesting as it shows that the red tail exhibits unusual thermal behavior. In light of these problems, we have further analyzed the thermal behavior of the red tail of the D1−D2−cyt*b*559 complex. We demonstrate that the unusual thermal behavior of the red tail is due to its marked temperature sensitivity, decreasing in intensity as the temperature is lowered, and that this may be explained in terms of low-energy vibrational bands associated with the weak coupling of electronic transitions (e.g., at 683 nm) to phonons of relatively high energy (80−150 cm^{-1}). Some of these data have been presented in a preliminary report (*21*).

MATERIALS AND METHODS

The D1−D2−cyt*b*559 complex was obtained according to the method of Chapman et al. (*3*), starting from PSII[1] membranes prepared as previously described (*20*). The absorption maximum at room temperature was close to 676 nm which is taken to be an indication that the complex is not degraded (*22*). Pigment analysis revealed a chlorophyll/pheophytin ratio of about 3 (*23*), thus indicating that the preparation used in this study is of the six-chlorophyll/two-pheophytin type.

Absorption spectra of the D1−D2−cyt*b*559 complex between 80 and 298 K were measured and numerically decomposed as previously described (*23*, *24*). The experimental spectra were fitted with a linear combination of Gaussian functions. Each Gaussian is defined as the sum of two half-Gaussians, thus allowing it to be asymmetrical. The absorption spectra thermal broadening was analyzed in the frame of the linear electron−phonon coupling assumption.

RESULTS

The D1−D2−cyt*b*559 complex spectroscopic properties are those of a heterogeneously broadened particle since different pigment-binding protein sites which alter the pigment energy levels exist, giving rise to different electronic transitions. The spectroscopic properties of the sub-bands are determined mostly by two types of contributions. The first is due to the coupling of the electronic transition to low-frequency vibrational modes (phonons) of the pigment−protein matrix, and its temperature dependence is determined by the occupation probability of these vibrational modes. This leads to the so-called "homogeneous" broadening of the absorption signal. The second is due to statistical fluctuations in the conformation of the chromophore binding site, and it is generally thought to be temperature-independent. This leads to the so-called "inhomogeneous" broadening. Thus, the mean square standard deviation (σ^2) of the absorption band of a pigment in a given site in the linear electron−phonon coupling assumption is given by ref *25*:

$$\sigma^2 = \sigma_{hom}^2 + \sigma_{inh}^2 = S\nu_m^2 \coth[(hc\nu_m)/(2k_BT)] + \sigma_{inh}^2 \quad (1)$$

where S and ν_m are the coupling strength and mean frequency (cm^{-1}) of the phonon bath, h is Planck's constant, c is the speed of light, k_B is the Boltzmann constant, T is the absolute temperature, and σ_{inh} is the contribution to σ (cm^{-1}) due to inhomogeneous broadening.

In the case of a composite absorption band, with N different electronic transitions the mean square standard deviation of the whole band (σ_{tot}) is given by (*26*)

$$\sigma_{tot}^2 = \sum_{k=1}^{N} A_k S_k \nu_{mk}^2 \coth[(hc\nu_{mk})/(2k_BT)] + \sigma'^2_{inh} \quad (2)$$

where A_k is the area of the kth absorption transition, $S_k\nu_{mk}$ is the optical reorganization energy for the kth transition, and σ'_{inh} is the contribution to σ_{tot} due to the inhomogeneous (statistical) broadening of each underlying transition and the broadening due to the presence of these different transitions (heterogeneity). For $hc\nu_{mk} \ll 2k_BT$, eq 2 can be simplified:

$$\sigma_{tot}^2 = C\sum_{k=1}^{N} A_k S_k \nu_{mk} T + \sigma'^2_{inh} \quad (3)$$

where $C = 1.39$ K^{-1} cm^{-1}. If it is assumed that all the underlying transitions have similar properties, plotting $(\sigma_{tot})^2$ of the absorption band as a function of temperature yields the $S\nu_m$ of the single transitions. When the underlying transitions have different electron−phonon coupling proper-

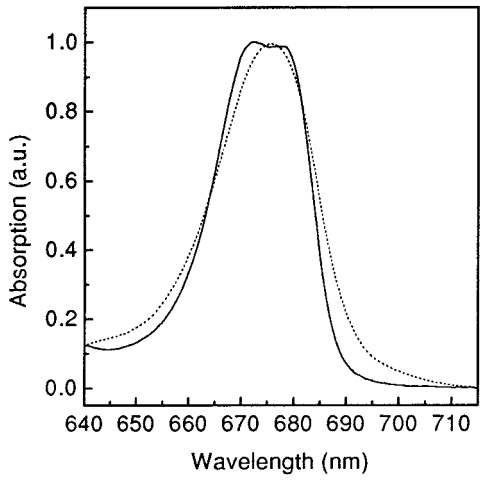

FIGURE 1: D1−D2−cyt*b*559 complex absorption spectra at room temperature (dotted line) and at 80 K (solid line).

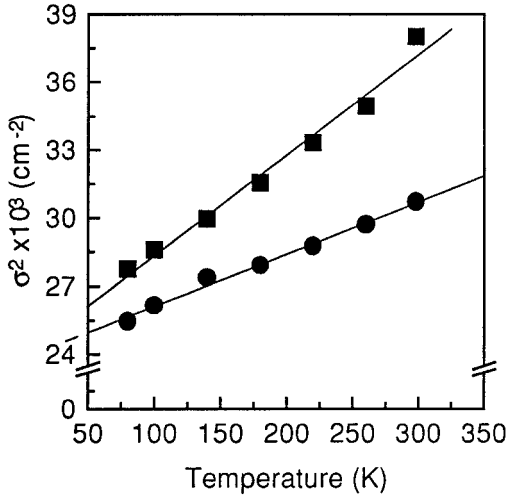

FIGURE 2: Temperature dependence of the $(\sigma_{tot})^2$ of the D1−D2−cyt*b*559 complex absorption spectrum. Data from the experimental spectrum (■) and data (●) after subtraction of long wavelength sub-bands in the case of two-sub-band tail decomposition, linear fit (solid lines).

Table 1: Average $S\nu_m$ Values Derived from Linear Fitting of the Temperature Dependence of the $(\sigma_{tot})^2$ of the D1−D2−cyt*b*559 Complex Experimental Absorption Spectrum[a]

	ES	ES − two red sub-bands	ES − three red sub-bands
$S\nu_m$ (cm^{-1})	32	16	20

[a] The values refer to analysis of the entire band (ES) and of the entire band from which either two or three of the minor red-most sub-bands were subtracted.

ties, the plot gives an average $S\nu_m$ for the various transitions which does not have a precise physical meaning.

Sample spectra are presented for room temperature and 80 K (Figure 1) where it can be seen that at the lower temperature the red edge goes to zero very abruptly, as is commonly observed. In the following, we analyze the σ^2 of the Q_y absorption band of the D1−D2−cyt*b*559 complex between 658 and 720 nm (see Figure 2 and Table 1) and from this determine, according to eq 3, an average $S\nu_m$ of 32 cm^{-1}. This value is much higher than that derived from studies of hole burning (*18*, *19*) and thermal broadening (*21*) of the single Gaussian sub-bands where, taking into account both P680 ($S\nu_m \approx 40$ cm^{-1}) and the accessory pigment transitions ($S\nu_m \approx 15-20$ cm^{-1}), average $S\nu_m$ values of around 20 cm^{-1} are expected for the total absorption band. In the remaining part of this analysis, we have investigated the possibility that this discrepancy might be associated with the red absorption tail, as it has already been noticed that this exhibits anomalous thermal behavior (see the introductory section).

The D1−D2−cyt*b*559 complex absorption spectrum was therefore decomposed into sub-bands as previously described (*20*; seven-sub-band decomposition) with the red tail being described by additional, minor, Gaussians. As we are only analyzing the red absorption tail in this study, the absence of the high-energy vibrational structure in our Gaussian model is not important. We note in passing that, as pointed out above, while it is possible to describe the thermal behavior of the red tail with an abnormally broad sub-band at 680 nm which has an unreasonably high apparent $S\nu_m$ (*20*), no such description is possible using a sub-band positioned at 683 nm, irrespective of the bandwidths employed (data not presented). Thus, for analytical purposes, we have used additional, minor Gaussians to describe the tail. Figure 3 shows two different decompositions describing the red tail, defined as the absorption signal not described by the sub-bands of the intense transitions at 680 and 683 nm which have thermal broadening characteristics (80−300 K) in agreement with hole burning (*7*, *13*) and selective photobleaching (*11*). In this way, the tail is described by either two or three sub-bands. For clarity, only the red half of the absorption spectra of the D1−D2−cyt*b*559 complex is shown in the figure. All the sub-bands which describe the absorption spectrum that are not in the red tail are identical to those already described (*20*); they are nearly symmetrical, and their peak positions and areas are conserved upon lowering *T*. On the other hand, when *T* is decreased, the sub-bands fitting the red tail tend to shift toward shorter wavelengths, and lose both height and area. No major difference is found among the two decompositions of the red tail. Both describe the absorption signal in this spectral region of the D1−D2−cyt*b*559 complex and its decrease on lowering the temperature. We emphasize here that no specific physical meaning is attributed to the sub-bands fitting the red absorption tail. They represent a way to analytically describe the anomalous thermal behavior of the red tail. When σ^2 for the absorption band was analyzed after subtraction of these minor, temperature sensitive, bands in the red tail, average $S\nu_m$ values between 16 and 20 cm^{-1} were obtained (Figure 2 and Table 1). Thus, the anomalous temperature behavior of the red tail seems indeed to be responsible for the large average apparent $S\nu_m$ obtained by analysis of the whole band.

DISCUSSION

In this paper, we analyze the thermal behavior of the red absorption tail of the D1−D2−cyt*b*559 complex which, as pointed out in the introductory section, seems to be anomalous. To this end, the red tail was studied (i) in terms of the mean square spectral deviation $(\sigma_{tot})^2$ of the entire Q_y absorption band of this complex as a function of *T* and (ii) by Gaussian decomposition. From this analysis of the mean

[1] Abbreviation: PSII, photosystem II.

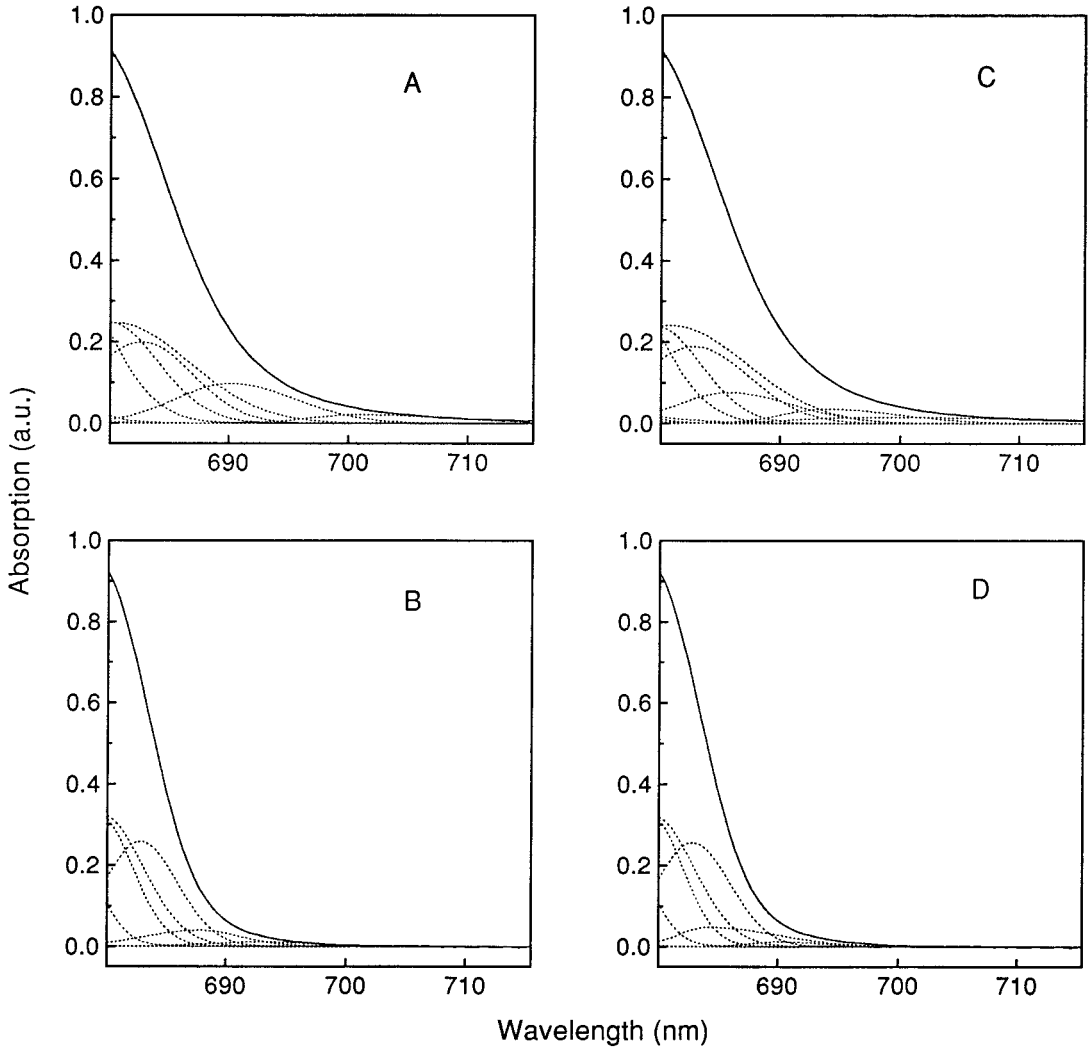

FIGURE 3: Gaussian decomposition analysis of the D1−D2−cyt*b*559 complex red absorption tail at room temperature (A and C) and 80 K (B and D). For clarity, only the red half of the absorption spectra (solid line) and the sub-bands peaking at 680 nm and longer wavelengths (dashed lines) are shown. The sum of the sub-bands is perfectly superimposed to the experimental curve and for this reason invisible. Panels A and B and C and D describe the red tail making use of either two or three sub-bands, respectively.

square spectral deviation, an average reorganization energy ($S\nu_m$) of 32 cm^{-1} was determined which, as described in the Results, is considerably greater than the expected value of around 20 cm^{-1}, determined on the basis of published values for P680 and the accessory pigments (*11*, *20*). This discrepancy was analyzed in terms of the thermal behavior of Gaussian sub-bands used to describe the red tail. The starting point for this analysis is the well-documented presence of absorption transitions near 680 and 683 nm (*5*, *7*, *13*) with characteristic electron−phonon coupling properties (*17*), which in the linear electron−phonon coupling assumption, lead to easily predicted thermal broadening behavior. The red tail is defined here as the long wavelength absorption signal which is not described by these two electronic transitions in the 80−300 K temperature interval and was analyzed in terms of two different sub-band descriptions, employing either two or three bands. In all cases, these minor sub-bands proved to have characteristics which were completely different from those of the major bands describing the spectral region outside the red tail. In particular, and this is not dependent on the number of sub-bands used, they are strongly asymmetrical at all temperatures and upon the temperature being lowered they shift toward shorter wavelengths and decrease in area. Interestingly, when σ^2 for the absorption band was calculated after subtraction of these minor, temperature sensitive red sub-bands, average $S\nu_m$ values of 16−20 cm^{-1} were calculated as expected (*11*, *20*). Thus, the unexpectedly high apparent reorganization energy of the whole band (32 cm^{-1}) is clearly due to the temperature sensitivity of the red tail.

We will now discuss the possible physical origin of the temperature sensitivity of the absorption red tail. From the extensive hole burning studies of protein-bound chlorophylls (*17*), apart from the low-frequency phonons with a ν_m of 20−30 cm^{-1}, weak Franck−Condon modes were also detected in the 200−500 cm^{-1} interval. As these modes are thermally accessible at room temperature, they will give rise to absorption bands on the low-energy side of the (0,0) transition. These absorption bands are, however, usually extremely weak, mainly because the higher-frequency phonons are only very weakly coupled to the chlorophyll electrons (*27*). On the other hand, recent site-selected fluorescence measurements (*19*, *28*) on the emitting state at 5 K of the D1−D2−cyt*b*559 complex seem to indicate the presence of an extensive vibrational structure in the frequency interval which is thermally accessible at room temperature, with a

pronounced and quite intense mode near 80 cm^{-1} suggesting a relatively high degree of coupling with the electronic transitions. These relatively high-frequency phonons are expected to give rise to a significant, low-energy, absorption vibrational structure at high temperatures which will decrease upon lowering the temperature (*26*) as does the red tail of the D1−D2−cyt*b*559 complex. We therefore tentatively conclude that the red tail of the PSII RC complex may not be due to electronic transitions but could be associated with low-energy vibrational bands, following the suggestion of Zucchelli et al. (*26*) for the red tail of LHCII. This conclusion could also explain the low-intensity Gaussian near 688 nm found in the decomposition analysis of the photobleaching at 80 K of the 683 nm spectral form in the D1−D2−cyt*b*559 complex (*11*).

In this hypothesis, the thermal broadening data (Figure 2) can be easily analyzed in terms of Franck−Condon coupling to both a low-frequency ($\nu_{mL} = 25$ cm^{-1}) and a high-frequency phonon (ν_{mH}) (*26*), which we have taken to be in the range of 80−150 cm^{-1}, according to

$$\sigma_{tot}^{2} = S_L \nu_{mL}^{2} \coth[(hc\nu_{mL})/(2k_BT)] + S_H \nu_{mH}^{2} \coth[(hc\nu_{mH})/(2k_BT)] + \sigma_{inh}^{2} \quad (4)$$

Using the values of ν_{mL} and ν_{mH} indicated above and an S_L of 0.7−1, we find values for S_H between 0.18 and 0.028, indicating that the electron−phonon coupling strength for coupling to the higher-frequency phonons is weaker than to the low-frequency phonon modes. Of course, if we had considered more than one high-frequency phonon in these calculations, the coupling strengths would have been even lower.

It should be pointed out that this analysis of thermal broadening absorption spectra contrasts with that of Peterman et al. (*19*). These authors discussed their site-selected fluorescence data, measured at 5 K, in terms of a strong "average" coupling ($S \cong 1.6$), for all vibrational modes in the 20−500 cm^{-1} interval, to the electronic transitions associated with the 680 and 683 nm forms. In passing, we point out that Groot et al. (*18*) considered that the P680 was nonfluorescent in the range of 2−4 K, so there are some unresolved discrepancies concerning the very low-temperature fluorescence measurements of this complex. We here show that the thermal broadening of the red tail can be well explained in terms of "strong" electron−phonon coupling ($S \cong 2$) for P680 to the low-frequency phonons, "weak" coupling ($S = 0.7-1.0$) of the 683 transition to the low-frequency bath, and "very weak" ($S = 0.028-0.18$) coupling of these transitions to higher-frequency phonons. Thus, we see no need to modify our previous conclusion (*11*), in agreement with that of Groot et al. (*18*), that the 683 nm transition has the electron−phonon coupling characteristics of a monomer, antenna-type chlorophyll.

REFERENCES

1. Wasielewski, M. R., Johnson, D. G., Seibert, M., and Govindjee (1992) *Proc. Natl. Acad. Sci. U.S.A. 86*, 524.
2. Roelofs, T. A., Gilbert, M., Shuvalov, A., and Holzwarth, A. R. (1991) *Biochim. Biophys. Acta 1060*, 237.
3. Chapman, D. J., Gounaris, K., and Barber, J. (1988) *Biochim. Biophys. Acta 933*, 423.
4. Seibert, M. (1993) in *The Photosynthetic Reaction Center* (Deisenhofer, J., and Norris, J., Eds.) Vol. 1, p 317, Academic Press, New York.
5. Chang, H. C., Jankowiak, R., Reddy, N. R. S., Yocum, C. F., Picorel, R., Seibert, M., and Small, G. J. (1994) *J. Phys. Chem. 98*, 7725.
6. Mimuro, M. (1993) *Plant Cell Physiol. 34*, 321.
7. Tang, D., Jankowiak, R., Seibert, M., Yocum, C. F., and Small, G. J. (1990) *J. Phys. Chem. 94*, 6519.
8. van der Vos, R., van Leeuwen, P. J., Braun, P., and Hoff, A. J. (1992) *Biochim. Biophys. Acta 1140*, 184.
9. Garlaschi, F. M., Zucchelli, G., Giavazzi, P., and Jennings, R. C. (1994) *Photosynth. Res. 41*, 465.
10. Witt, H. T., Schlodder, E., Brettel, K., and Saygin, O. (1986) *Ber. Bunsen-Ges. Phys. Chem. 90*, 1015.
11. Finzi, L., Elli, G., Zucchelli, G., Garlaschi, F. M., and Jennings R. C. (1998) *Biochim. Biophys. Acta 1366*, 256.
12. den Hartog, F. T. H., Vacha, F., Lock, A. J., Barber, J., Dekker, J. P., and Volker, S. (1998) *J. Phys. Chem. B 102*, 9174.
13. Kwa, S. L. S., Eijckelhoff, R., van Grondelle, R., and Dekker, J. P. (1994) *J. Phys. Chem. 98*, 7702.
14. Konermann, L., Yruela, I., and Holzwarth, A. R. (1997) *Biochemistry 36*, 7498.
15. Tetenkin, V. I., Gulyaev, B. A., Seibert, M., and Rubin, A. B. (1989) *FEBS Lett. 250*, 459.
16. Durrant, J. R., Klug, D. R., Kwa, S. L. S., van Grondelle, R., and Dekker, J. P. (1995) *Proc. Natl. Acad. Sci. U.S.A. 92*, 15267.
17. Johnson, S. G., Lee, I., and Small, G. J. (1991) in *Chlorophylls* (Sheer, H., Ed.) pp 739−768, CRC Press, Boca Raton, FL.
18. Groot, M. L., Dekker, J. P., van Grondelle, R., den Hartog, F. T. H., and Volker, S. (1996) *J. Phys. Chem. 100*, 11488.
19. Peterman, E. J., van Amerongen, H., van Grondelle, R., and Dekker, J. P. (1998) *Proc. Natl. Acad. Sci. U.S.A. 95*, 6128.
20. Cattaneo, R., Zucchelli, G., Garlaschi, F. M., Finzi, L., and Jennings R. C. (1995) *Biochemistry 34*, 15267.
21. Finzi, L., Elli, G., Garlaschi, F. M., Zucchelli, G., and Jennings, R. C. (1998) in *Photosynthesis: Mechanisms and Effects* (Garab, G., Ed.) p 1077, Kluwer Academic Publishers, Dordrecht, The Netherlands.
22. Booth, P. J., Crystall, B., Ahmed, I., Barber, J., Porter, G., and Klug, D. R. (1991) *Biochemistry 30*, 7573.
23. Zucchelli, G., Garlaschi, F. M., Croce, R., Bassi, R., and Jennings, R. C. (1995) *Biochim. Biophys. Acta 1229*, 59.
24. Jennings, R. C., Bassi, R., Garlaschi, F. M., Dainese, P., and Zucchelli, G. (1993) *Biochemistry 32*, 3203.
25. Hayes, J. M., Gillie, J. K., Tang, D., and Small, G. J. (1988) *Biochim. Biophys. Acta 932*, 287.
26. Zucchelli, G., Garlaschi, F. M., and Jennings, R. C. (1996) *Biochemistry 35*, 16247.
27. Zucchelli, G., Cremonesi, O., Garlaschi, F. M., and Jennings, R. C. (1998) in *Photosynthesis: Mechanisms and Effects* (Garab, G., Ed.) p 449, Kluwer Academic Publishers, Dordrecht, The Netherlands.
28. den Hartog, F. T. H., Dekker, J. P., van Grondelle, R., and Volker, S. (1998) *J. Phys. Chem. B 102*, 11007.

BI990568O